LETTER

doi:10.1038/nature11188

The limits of the nuclear landscape

Jochen Erler[1,2], Noah Birge[1], Markus Kortelainen[1,2,3], Witold Nazarewicz[1,2,4], Erik Olsen[1,2], Alexander M. Perhac[1] & Mario Stoitsov[1,2]‡

In 2011, 100 new nuclides were discovered[1]. They joined the approximately 3,000 stable and radioactive nuclides that either occur naturally on Earth or are synthesized in the laboratory[2,3]. Every atomic nucleus, characterized by a specific number of protons and neutrons, occupies a spot on the chart of nuclides, which is bounded by 'drip lines' indicating the values of neutron and proton number at which nuclear binding ends. The placement of the neutron drip line for the heavier elements is based on theoretical predictions using extreme extrapolations, and so is uncertain. However, it is not known how uncertain it is or how many protons and neutrons can be bound in a nucleus. Here we estimate these limits of the nuclear 'landscape' and provide statistical and systematic uncertainties for our predictions. We use nuclear density functional theory, several Skyrme interactions and high-performance computing, and find that the number of bound nuclides with between 2 and 120 protons is around 7,000. We find that extrapolations for drip-line positions and selected nuclear properties, including neutron separation energies relevant to astrophysical processes, are very consistent between the models used.

Only 288 of the several thousand nuclides, or isotopes, known to inhabit the nuclear landscape are either stable or practically stable (that is, have half-lives longer than the expected life of the Solar System). These 288 nuclides form the 'valley of stability' (Fig. 1). By moving away from this valley, by adding nucleons, we enter the vast territory of short-lived radioactive nuclei, which disintegrate by emitting β- and α-particles or split into smaller parts through spontaneous fission. Nuclear existence ends at the drip lines, where there is no longer enough binding energy to prevent the last nucleons from escaping the nucleus. As indicated in Fig. 1, the proton-rich border of the nuclear territory has been experimentally delineated up to protactinium[2] (proton number, $Z = 91$). The neutron-rich boundary is known only up to oxygen ($Z = 8$) because of the long distance separating the valley of stability from the neutron drip line[3]. The superheavy nucleus with $Z = 118$ and $A = 294$ (ref. 4) marks the current limit of nuclear charge and mass. The borders of the superheavy region are unknown and difficult to predict because competition between Coulomb and shell effects can cause voids and exotic topologies to form (compare with section 4 of ref. 5).

Today, about 3,000 nuclides are known[2,3] (see also http://www.nscl.msu.edu/~thoennes/2009/discovery.htm). Experimental exploration of very neutron-rich nuclei is extremely challenging because of the very low production rates in studies involving the fragmentation of stable nuclei, and the separation and identification of the products. It is anticipated that the next generation of radioactive ion-beam facilities will have high-power beams and highly efficient and selective fragment separators with which to delineate most of the neutron drip line up to mass number $A \approx 100$ (ref. 6).

The primary factor that determines the particle stability—and drip line—of a nuclide is its separation energy[3]: the amount of energy needed to remove from it a single neutron (S_{1n}) or proton (S_{1p}) or two neutrons (S_{2n}) or protons (S_{2p}). In terms of the binding energy, $B(Z,N)$, where N denotes the neutron number, the one-neutron and two-neutron separation energies are $S_{1n}(Z,N) = B(Z,N-1) - B(Z,N)$ and $S_{2n}(Z,N) = B(Z,N-2) - B(Z,N)$, respectively; analogous relationships apply to protons. If the separation energy is positive, the nucleus is stable to nucleon emission; conversely, if the separation energy is negative, the nucleus is unstable. The drip line is reached when $S_{1n} \approx 0$ (one-neutron drip line) or $S_{2n} \approx 0$ (two-neutron drip line). The drip-line position is strongly affected by nucleonic superfluidity[7], which makes nuclei with even numbers of nucleons more bound than their odd-nucleon-number neighbours. In terms of the chemical potential, λ_n, and odd–even energy difference (or pairing gap), Δ_n, the separation energies can be written[8] as $S_{1n} \approx -\lambda_n - \Delta_n$ (for odd N) and $S_{2n} \approx -2\lambda_n$ (for even N). Although the negative chemical potential guarantees that an even-N system is bound, this is not true if N is odd: $S_{1n} > 0$ only if $\lambda_n < -\Delta_n$. The helium isotopes provide evidence for the impact of pairing on nuclear existence: the even–even isotopes ^{4}He, ^{6}He and ^{8}He are bound whereas ^{5}He, ^{7}He and ^{9}He are not. Consequently, the one-nucleon drip line is reached earlier than the two-nucleon drip line, and the region of nuclear existence has a ragged border that zigzags between odd- and even-particle species. Because the aim of this study is to estimate the maximum extent of nuclear binding, we focus on even–even nuclei and two-neutron separation energies.

The quest for the limits of nuclear binding is closely connected to the question about the origin of elements in the universe. The astrophysical rapid proton capture and rapid neutron capture processes, which are responsible for the generation of many heavy elements, operate very close to the drip lines[9]; hence, the structure of very exotic, weakly bound nuclei directly impacts the way the elements are produced in stars.

From the theoretical point of view, the description of weakly bound superfluid complex nuclei is a demanding task as it requires the understanding and control of three crucial aspects of the nuclear many-body problem: interaction, pairing and coupling to the low-lying particle continuum[10,11]. For such a task, the microscopic tool of choice is the nuclear density functional theory (DFT) based on the self-consistent mean-field approach[12]. The main ingredient of the nuclear DFT is the effective interaction between nucleons represented by the energy density functional (EDF), which depends on total (neutron-plus-proton) and isovector (neutron-minus-proton) densities and currents. Because the coupling constants of the nuclear EDF cannot yet be computed by *ab initio* methods, it is customary to use optimization techniques to adjust them to carefully selected experimental data[13–15] (primarily on nuclei near the valley of stability). The resulting uncertainties in model parameters can be used to estimate statistical errors of calculated quantities, especially when it comes to extrapolations into unexplored regions (for example towards the neutron drip line)[14]. However, to estimate systematic model errors, resulting from different theoretical assumptions and/or different optimization protocols, it is necessary to compare a variety of models and parameterizations. In this way, it is possible to assess the robustness of theoretical predictions and estimate theoretical uncertainties. The

[1]Department of Physics and Astronomy, University of Tennessee, Knoxville, Tennessee 37996, USA. [2]Physics Division, Oak Ridge National Laboratory, Oak Ridge, Tennessee 37831, USA. [3]Department of Physics, PO Box 35 (YFL), University of Jyväskylä, FI-40014 Jyväskylä, Finland. [4]Institute of Theoretical Physics, Warsaw University, PL-00681 Warsaw, Poland.
‡Deceased.

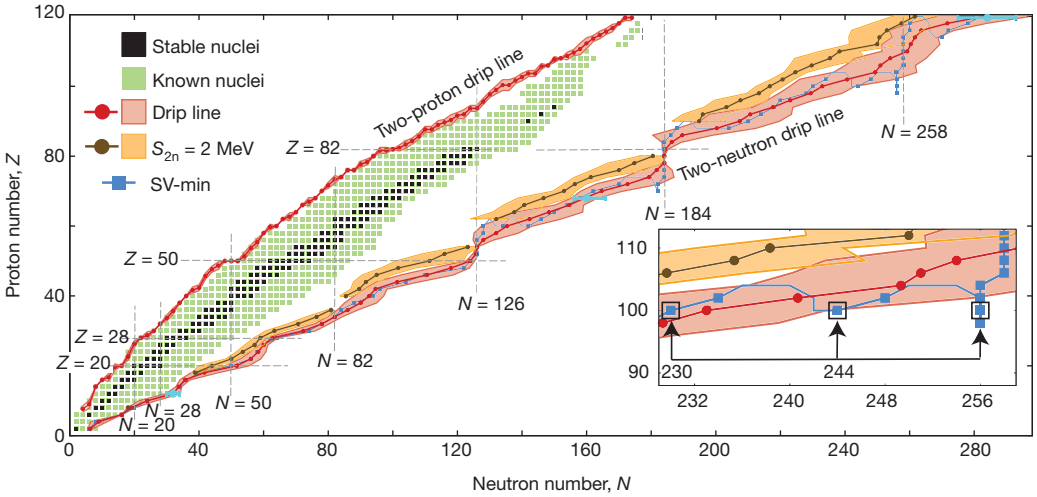

Figure 1 | Nuclear even–even landscape as of 2012. Map of bound even–even nuclei as a function of Z and N. There are 767 even–even isotopes known experimentally,[2,3] both stable (black squares) and radioactive (green squares). Mean drip lines and their uncertainties (red) were obtained by averaging the results of different models. The two-neutron drip line of SV-min (blue) is shown together with the statistical uncertainties at $Z = 12$, 68 and 120 (blue error bars). The $S_{2n} = 2$ MeV line is also shown (brown) together with its systematic uncertainty (orange). The inset shows the irregular behaviour of the two-neutron drip line around $Z = 100$.

application of modern optimization and statistical methods, together with high-performance computing, has revolutionized nuclear DFT during recent years.

In our study, we use quasi-local Skyrme functionals[15] in the particle–hole channel augmented by the density-dependent, zero-range pairing term. The commonly used Skyrme EDFs reproduce total binding energies with a root mean square error of the order of 1–4 MeV (refs 15, 16), and the agreement with the data can be significantly improved by adding phenomenological correction terms[17]. The Skyrme DFT approach has been successfully tested over the entire chart of nuclides on a broad range of phenomena, and it usually performs quite well when applied to energy differences (such as S_{2n}), radii and nuclear deformations. Other well-calibrated mass models include the microscopic–macroscopic finite-range droplet model (FRDM)[18], the Brussels–Montreal Skyrme–HFB models based on the Hartree–Fock–Bogoliubov (HFB) method[17] and Gogny force models[19,20].

Figure 2 illustrates the difficulties with theoretical extrapolations towards drip lines. Shown are the S_{2n} values for the isotopic chain of even–even erbium isotopes predicted with different EDF, SLy4[21], SV-min[13], UNEDF0[15], UNEDF1[22], and with the FRDM[18] and HFB-21[17] models. In the region for which experimental data are available, all models agree and well reproduce the data. However, the discrepancy between various predictions steadily grows when moving away from the region of known nuclei, because the dependence of the effective force on the neutron-to-proton asymmetry (neutron excess) is poorly determined. In the example considered, the neutron drip line is

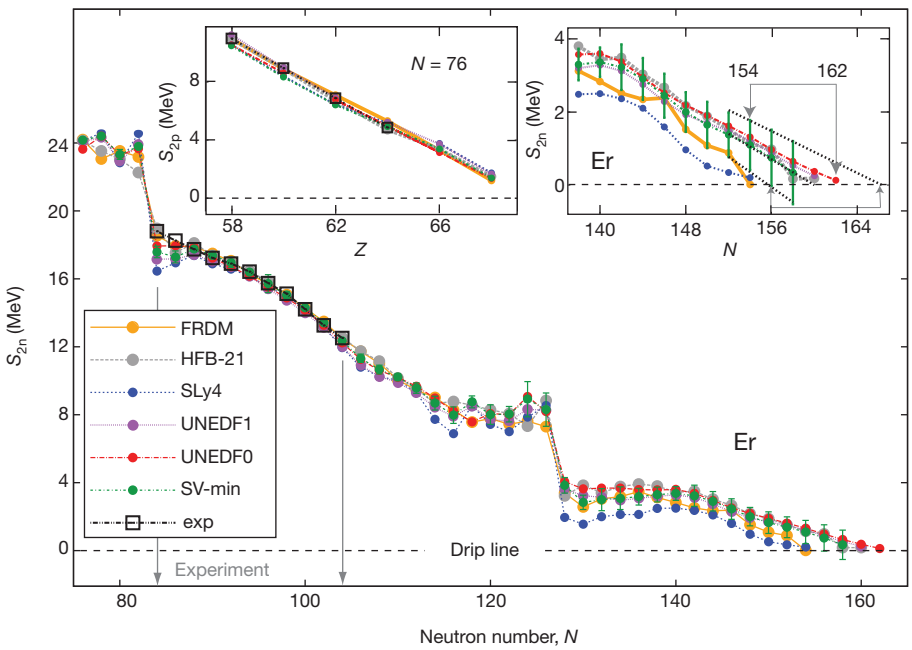

Figure 2 | Calculated and experimental two-neutron separation energies of even–even erbium isotopes. Calculations performed in this work using SLy4, SV-min, UNEDF0 and UNEDF1 functionals are compared to experiment[2] and FRDM[18] and HFB-21[17] models. The differences between model predictions are small in the region where data exist (bracketed by vertical arrows) and grow steadily when extrapolating towards the two-neutron drip line ($S_{2n} = 0$). The bars on the SV-min results indicate statistical errors due to uncertainty in the coupling constants of the functional. Detailed predictions around $S_{2n} = 0$ are illustrated in the right inset. The left inset depicts the calculated and experimental two-proton separation energies at $N = 76$.

predicted to be between $N = 154$ (FRDM) and $N = 162$ (UNEDF0); that is, the model-dependent 'error bar' is appreciable. This is not the case for the proton-rich boundary. The calculated values of S_{2p} at $N = 76$ are shown in the left inset of Fig. 2. Because the proton drip line lies relatively close to the valley of stability owing to the repulsive electrostatic interaction between protons, and because the proton continuum is effectively shifted up in energy as a result of the confining effect of the Coulomb barrier, the associated extrapolation error is small and all the models we used are in excellent agreement with experiment.

As discussed earlier, in addition to systematic errors, calculated observables are also subject to statistical errors due to uncertainties in EDF parameters[13,14]. Fig. 2 shows how the statistical error in S_{2n} predicted with the SV-min EDF propagates with N. The gradual growth of error bars when approaching the neutron drip line is primarily caused by the isovector coupling constants of the functional that are not well constrained by the current data[14]. The resulting statistical error in the position of the neutron drip line can be obtained by extrapolating the error band of calculated values towards $S_{2n} = 0$ (indicated by dotted lines in the right inset of Fig. 2). In the case of SV-min and erbium isotopes, the statistical uncertainty corresponds to $N = 156$–166.

To assess the current status of theoretical predictions for the limits of nuclear binding and provide a benchmark for future improvements, we carried out large-scale DFT calculations[16,23] of global nuclear properties using six Skyrme EDFs (SkM*[24], SkP[25], SLy4[21], SV-min[13], UNEDF0[15] and UNEDF1[22]) and covering a wide range of even–even nuclei of up to 120 protons and 300 neutrons. The summary of our survey is presented in Fig. 1. The dashed grey gridlines show the magic numbers known around the valley of stability (20, 28, 50, 82 and 126) as well as the predicted regions of stability in superheavy nuclei[6] around $N = 184$ and 258. The mean neutron and proton drip lines and associated systematic uncertainties have been obtained by averaging the predictions of individual models (given in tabular form in Supplementary Information). We also show the two-neutron drip line of SV-min together with its statistical error bars at $Z = 12$, 68, and 120. As can be seen, the statistical error generally falls into the band of systematic uncertainty.

As expected, the theoretical error in the position of the neutron drip line grows steadily with distance from the valley of stability. Yet the overall consistency of model predictions is greater than initially anticipated. This is particularly true for $N \leq 50$ and N around 60, 126 and 184, where the error band is small. In particular, the recently discovered isotope ^{40}Mg (ref. 26) is predicted to be neutron-bound by all our models. Also, the neutron-rich isotopes ^{26}O and ^{28}O are consistently calculated to lie inside the neutron drip line. Experimental searches have so far provided no evidence[3] for the existence of ^{26}O and ^{28}O, and configuration interaction calculations[27] have attributed this anomalous behaviour to the repulsive three-body force. If a similar effect is observed in heavier nuclei, where DFT calculations are believed to be more reliable, this may suggest systematic modifications of the isovector-density-dependent interactions of EDF. As illustrated in Supplementary Fig. 1, the predictions of the FRDM and HFB-21 models generally fall within our uncertainty band.

As seen in Fig. 1, the two-neutron drip line has a complicated zigzag pattern in some regions. The inset shows the irregular behaviour of the two-neuron drip line predicted by SV-min at around $Z = 100$. Although the primary drip line is located at $N = 230$, neutron binding reappears around $N = 242$ and then again at $N = 256$, giving rise to a secondary and a tertiary drip line. Such behaviour is due to the presence of shell effects at neutron closures that tend to lower binding energy along the localized bands of stability[16]. The phenomenon of re-entrant binding is predicted in several areas of the neutron drip line, for example at around $Z = 60$ ($N = 132$ and 140), 70 ($N = 182$) and 100 ($N = 258$). (For more examples, see Supplementary Information and also refs 16–20.)

The astrophysical rapid neutron capture process (r-process) is expected to proceed along a path of constant neutron separation energies, fairly close to the neutron drip line[9]. Fig. 1 shows the $S_{2n} = 2$ MeV line, together with its uncertainty band, corresponding to the very neutron-rich r-process path. (Such theoretical data can be used in future r-process simulations to estimate uncertainties of element abundances related to theoretical uncertainties of separation energies; on request, we can provide uncertainties for other values of S_{2n} and S_{1n}.) Again, the DFT predictions seem fairly robust, especially around the neutron magic numbers where the separation energies change rapidly. Finally, there is a great deal of consistency between models regarding the position of the two-proton drip line, with the calculated systematic uncertainty usually not exceeding $\Delta Z = 2$. The nuclides ^{42}Cr, ^{48}Ni and ^{54}Zn, which are known[2] to be two-proton unstable, are firmly predicted as such, as are the α-emitters ^{166}Pt, ^{172}Hg and ^{186}Po.

To assess how model dependent DFT extrapolations are when it comes to observables other than the separation energy, in Supplementary Figs 2–4 we show the mass and isovector quadrupole deformations and differences between radii of neutron and proton distributions (neutron skins) predicted in our models. Despite the fact that these quantities are greatly influenced by shell effects, global patterns predicted by various EDFs are fairly similar.

The intermodel consistency of our results allows us to address the question of the number of isotopes inhabiting the nuclear landscape. According to our Skyrme DFT mass tables, the numbers of particle-bound even–even nuclei with $2 \leq Z \leq 120$ are 2,333 in the SkM* model, 2,042 in SkP, 1,928 in SLy4, 2,116 in SV-min, 2,209 in UNEDF0 and 2,219 in UNEDF1. Adding the odd-mass and odd–odd neighbours, we predict that $6{,}900 \pm 500_{syst}$ nuclei with $Z \leq 120$ are bound to proton and neutron emission. To put things in perspective, the total number of nuclides known experimentally is slightly more than 3,000 (refs 1, 2). Although the majority of rare isotopes inhabiting the outskirts of the nuclear landscape are unlikely to be seen, their properties impact astrophysical processes and, hence, the matter around us. The road to understanding those exotic species takes us through reliable nuclear simulations with quantified uncertainties, and this study represents a step in this direction. In the long term, of particular importance is the development of novel nuclear energy density functionals that reproduce both bulk nuclear properties and spectroscopic data. Work along these lines is in progress[15,22].

The experimental range of the nuclear landscape is fluid: new rare isotopes are being added to it every year. As experiment advances, increasingly more-quantitative models of the atomic nucleus are being developed with the aid of high-performance computing. In this context, the theoretical range of the chart of nuclides is continually changing, and our predictions should be viewed as specific to 2012.

METHODS SUMMARY

The calculations were carried out within the nuclear DFT framework[16,23]. The Skyrme functionals SkM*[24], SkP[25], SLy4[21], SV-min[13], UNEDF0[15] and UNEDF1[22] were used in the particle–hole channel, and a density-dependent pairing force of the mixed type[28] was used in the pairing channel. The self-consistent HFB equations of the nuclear DFT were solved with the code HFBTHO[29] as further optimized in refs 15, 22. The code solves the nonlinear HFB equations in configuration space by expanding self-consistent eigenstates in a large basis of the deformed harmonic oscillator. The axial symmetry and parity of nuclear mean fields are imposed to reduce the dimension and complexity of the problem. (The effect of triaxial and reflection-asymmetric ground-state deformations on particle drip lines is expected to be minor[30].) The single-particle basis consisted of the harmonic oscillator states originating in the 20 major oscillator shells (see Supplementary Fig. 5 and Supplementary Information for more discussion). To restore approximately the particle number symmetry broken in HFB, we used the variant of the Lipkin–Nogami scheme in ref. 16. The large-scale mass tables were computed using the JAGUAR and KRAKEN Cray XT5 supercomputers housed at Oak Ridge National Laboratory.

The Skyrme energy functional with a pairing term is parameterized by up to 14 coupling constants. To assess better the systematic error, we used functionals having distinct characteristics. SkM* was developed with a focus on surface energy

and fission barriers; SkP aimed at a simultaneous description of the mean field and pairing; SLy4 was optimized with a bias on neutron-rich nuclei and properties of neutron matter; SV-min was adjusted to a variety of data on spherical nuclei, including diffraction radii and surface thickness; UNEDF0 was developed by considering data on spherical and deformed nuclei; and the data set of UNEDF1 also considered excitation energies of fission isomers.

Received 28 February; accepted 2 May 2012.

1. Thoennessen, M. & Sherrill, B. From isotopes to the stars. *Nature* **473,** 25–26 (2011).
2. National Nuclear Data Center. Evaluated Nuclear Structure Data File. http://www.nndc.bnl.gov/ensdf/.
3. Thoennessen, M. Reaching the limits of nuclear stability. *Rep. Prog. Phys.* **67,** 1187–1232 (2004).
4. Oganessian, Yu Ts. *et al.* Synthesis of the isotopes of elements 118 and 116 in the ^{249}Cf and ^{245}Cm+^{48}Ca fusion reactions. *Phys. Rev. C* **74,** 044602 (2006).
5. Nazarewicz, W. *et al.* Theoretical description of superheavy nuclei. *Nucl. Phys. A* **701,** 165–171 (2002).
6. Rare Isotope Science Assessment Committee. *Scientific Opportunities with a Rare-Isotope Facility in the United States* (Natl Acad. Press, 2007).
7. Brink, D. M. & Broglia, R. A. *Nuclear superfluidity: pairing in finite systems* (Cambridge Univ. Press, 2005).
8. Beiner, M., Lombard, R. J. & Mas, D. Self-consistent calculations of ground state properties for unstable nuclei. *Nucl. Phys. A* **249,** 1–28 (1975).
9. Langanke, K. & Wiescher, M. Nuclear reactions and stellar processes. *Rep. Prog. Phys.* **64,** 1657–1701 (2001).
10. Dobaczewski, J. *et al.* Shell structure of exotic nuclei. *Prog. Part. Nucl. Phys.* **59,** 432–445 (2007).
11. Matsuo, M. & Nakatsukasa, T. Open problems in nuclear structure near drip lines. *J. Phys. G* **37,** 064017 (2010).
12. Bender, M., Heenen, P.-H. & Reinhard, P.-G. Self-consistent mean-field models for nuclear structure. *Rev. Mod. Phys.* **75,** 121–180 (2003).
13. Klüpfel, P. *et al.* Variations on a theme by Skyrme: a systematic study of adjustments of model parameters. *Phys. Rev. C* **79,** 034310 (2009).
14. Reinhard, P.-G. & Nazarewicz, W. Information content of a new observable: The case of the nuclear neutron skin. *Phys. Rev. C* **81,** 051303(R) (2010).
15. Kortelainen, M. *et al.* Nuclear energy density optimization. *Phys. Rev. C* **82,** 024313 (2010).
16. Stoitsov, M. V. *et al.* Systematic study of deformed nuclei at the drip lines and beyond. *Phys. Rev. C* **68,** 054312 (2003).
17. Goriely, S., Chamel, N. & Pearson, J. M. Further explorations of Skyrme-Hartree-Fock-Bogoliubov mass formulas. XII. Stiffness and stability of neutron-star matter. *Phys. Rev. C* **82,** 035804 (2010).
18. Möller, P. *et al.* Nuclear ground-state masses and deformations. *At. Data Nucl. Data Tables* **59,** 185–381 (1995).
19. Goriely, S., Hilaire, S., Girod, M. & Peru, S. First Gogny-Hartree-Fock-Bogoliubov nuclear mass model. *Phys. Rev. Lett.* **102,** 242501 (2009).
20. Delaroche, J.-P. *et al.* Structure of even-even nuclei using a mapped collective Hamiltonian and the D1S Gogny interaction. *Phys. Rev. C* **81,** 014303 (2010).
21. Chabanat, E. *et al.* A Skyrme parametrization from subnuclear to neutron star densities Part II. Nuclei far from stabilities. *Nucl. Phys. A* **635,** 231–256 (1998); erratum **643,** 441 (1998).
22. Kortelainen, M. *et al.* Nuclear energy density optimization: large deformations. *Phys. Rev. C* **85,** 024304 (2012).
23. Stoitsov, M., Nazarewicz, W. & Schunck, N. Large-scale mass table calculations. *Int. J. Mod. Phys. E* **18,** 816–822 (2009).
24. Bartel, J. *et al.* Towards a better parametrisation of Skyrme-like effective forces: a critical study of the SkM force. *Nucl. Phys. A* **386,** 79–100 (1982).
25. Dobaczewski, J., Flocard, H. & Treiner, J. Hartree-Fock-Bogolyubov description of nuclei near the neutron-drip line. *Nucl. Phys. A* **422,** 103–139 (1984).
26. Baumann, T. *et al.* Discovery of ^{40}Mg and ^{42}Al suggests neutron drip-line slant towards heavier isotopes. *Nature* **449,** 1022–1024 (2007).
27. Otsuka, T. *et al.* Three-body forces and the limit of oxygen isotopes. *Phys. Rev. Lett.* **105,** 032501 (2010).
28. Dobaczewski, J., Nazarewicz, W. & Stoitsov, M. V. Nuclear ground-state properties from mean-field calculations. *Eur. Phys. J. A* **15,** 21–26 (2002).
29. Stoitsov, M. V. *et al.* Axially deformed solution of the Skyrme–Hartree–Fock–Bogolyubov equations using the transformed harmonic oscillator basis. The program HFBTHO (v1.66p). *Comput. Phys. Commun.* **167,** 43–63 (2005).
30. Möller, P. *et al.* Axial and reflection asymmetry of the nuclear ground state. *At. Data Nucl. Data Tables* **94,** 758–780 (2008).

Supplementary Information is linked to the online version of the paper at www.nature.com/nature.

Acknowledgements This work was supported by the Office of Nuclear Physics, US Department of Energy, and by the Academy of Finland.

Author Contributions Theoretical calculations were performed by J.E., M.K. and M.S. The data were analysed by N.B., J.E., W.N., E.O. and A.M.P. The manuscript was prepared by J.E. and W.N. All authors contributed to this work, discussed the results and conclusions, and commented on the manuscript.

Author Information Reprints and permissions information is available at www.nature.com/reprints. The authors declare no competing financial interests. Readers are welcome to comment on the online version of this article at www.nature.com/nature. Correspondence and requests for materials should be addressed to W.N. (witek@utk.edu)